Journal of Solar Energy Research (JSER)

JSER

Presenting a New High Gain Boost Converter with Inductive Coupling Energy Recovery Snubber for Renewable Energy Systems- Simulation, Design and Construction

Omid Sharifiyana[a,b], Majid Dehghani[a,b*], Ghazanfar Shahgholian[a,b*], Sayyed Mohammad Mehdi Mirtalaei[a,b]

[a] *Department of Electrical Engineering, Najafabad Branch, Islamic Azad University, Najafabad, Iran*
[b] *Smart Microgrid Research Center, Najafabad Branch, Islamic Azad University, Najafabad, Iran*

ARTICLE INFO

ABSTRACT

Solar energy is one of the most important sources of energy because it is a renewable and inexhaustible energy. This paper presents a new energy recovery snubber for a high step-up boost converter, which can be used in renewable energy systems such as photovoltaic. The proposed snubber enjoys useful advantages such as providing soft-switching conditions, high voltage gain, simplicity of control, and balanced voltage stresses. In this topology, the voltage stress on the diodes and switches is a small percentage of the output voltage. A simple boost and a fly-forward converter are used to increase the output voltage. A snubber circuit is used for the main switch to recover the energy of the snubber capacitor. Therefore, the main switch turns off at low voltage and it causes a reduction in turn off loss. Experimental results of a 48V to 380V and 500W laboratory prototype show efficiency greater than 95% and verify the given theoretical analysis.

1. Introduction

In most renewable energy sources, the voltage level provided by the transducer is too low [1,2]. Employing a galvanic transformer not only increases the converter cost but also reduces the power density [3,4].

*Corresponding Author Email: dehghani@pel.iaun.ac.ir and shahgholian@iaun.ac.ir

A high step-up boost converter has been successfully utilized as a switching topology to enhance the system power density [5,6]. Today, the use of renewable energy to produce electrical energy is very important [7,8]. These plants do not have environmental problems, but in these power plants, the output voltage is low. Therefore, high step-up converters are used to increase the output voltage of renewable energy plants [9,10]. DC/DC boost converters are divided into several categories, such as isolated converters, non-isolated converters, and ETC [11,12]. In isolated converters, the input and output voltages are connected with a magnetic coupling and in non-isolated converters, there are electrical connections between the input and output voltage [13,14]. In non-isolated, high-step-up, low-cost, and high-efficiency front-end dc/dc converters are necessary due to the high-power-density requirements in renewable grid-connected applications [15,16]. The non-isolated high-step-up converters are included in several categories [17,18]. The conventional interleaved boost converter combined with a diode-capacitor. This converter is useful for high voltage gain and other converters that are based on the same topology [19,20]. The active circuit for soft switching has reduced the switching losses of conventional converters and similar topologies [21,22]. The input inductors of the conventional interleaved boost converter can be integrated into one coupled inductor to reduce the magnetic components. The output-diode reverse recovery problem can be alleviated, and zero current switching (ZCS) turn-on of the switches can be achieved due to the leakage inductance of the coupled inductor [23,24]. Other non-isolated boost converters are three-level boost converters. A three-level boost converter can double the output voltage of the converter and can halve the voltage stress of the power device compared to a conventional two-level boost converter [25,26]. The voltage gain of conventional boost converters and three-level boost converters is lower than the voltage level required in many applications requiring high voltages. Conventional boost converters and three-level boost converters with an improved cascade structure. The current ripple can be further reduced and the voltage gain can be increased to make the high step requirements possible by using a cascade structure [27,28]. To optimize and increase productivity, low cost, and high efficiency in power grid-connected PV applications, many researchers are paying close attention to how the above steps are accomplished, at the lowest cost [29,30]. Converters in this field are: step-up converters with switched capacitors [31,32], high-step converters with inductors and switched capacitors [33,34], high-step converters with coupled inductors [35,36], etc.

One of the most popular top-level converter topologies is inductor-based converters. Connecting or tapping the inductor is a convenient, useful and practical way to achieve wide voltage conversion ratios [37]. The fly-back and fly-forward converters are two main topologies of magnetic coupler converters. Coupled inductors topologies are the most popular in high step up converters. Adding the main switch duty cycle, the active clamp circuits have increased the output voltage in the fly-back converters [38]. The fly-back converters with output clamp circuit can reduce output current ripple and improve voltage gain [39]. In order to optimize the fly-back converters, new structures with multi-level capacitors on the secondary side have greatly helped to reduce the voltage stress and improve the voltage gain of the converter [40]. A very detailed mathematical calculation for a passive snubber in fly-back circuits is given in [41] which can be useful for adapting many new ideas. Active snubber circuits with a smart magnetic combination in a fly-back converter can help to improve the voltage gain of the converter in addition to playing a role in reducing switching losses [42].

The resonant structure combined with the active snubber circuit will provide the designer with a suitable topology to reduce losses and voltage stresses, although frequency and load limitations are an integral part of such techniques [43]. In fly-back converters, the snubber circuit or inductor-resonance or path are conventional methods used to reduce switching losses of converters. These methods, in addition to reducing the output current ripple, minimize the switching losses of the converter and increase the voltage gain of the converter [44]; The snubber circuits and inductor resonance have increased the converter efficiency and reduced switching losses but the inductor resonance has limited the converter operating frequency [45]. The half-bridge boost converter with a snubber capacitor, increases the converter voltage gain and reduces switching losses, but in this topology the energy is lost in the capacity there will be lost [46]. In this category, the attractive topology of improved efficiency performance and voltage gain of quasi-resonant passive snubber circuit should not be ignored [47]. The diode-capacitor-resistor snubber circuit is a common and simple technique to reduce the voltage stress on the switch in the low-pressure side bidirectional converters, although such a structure imposes relatively high internal losses on the converter [48].

The voltage gain of the fly-back and fly-forward converter [49].

In the passive hybrid structure in snubber circuits, in order to restore the power stored in the snubber capacitor, the designers of receiver circuits use snubber structures. This must cover different demands, including controllability, minimal load dependence, simple implementation, usable in different topologies without the need for a bulky and expensive converter, etc [50]. A classification of many basic techniques using snubber circuits, both active and passive snubber circuits that can be used in fly-back-based boost converters, is categorized in [51], which is omitted to avoid repetition.

The fly-forward converters have high voltage gain and the converter output current is continuously compared to fly-back converters. There are several sub-categories of fly-forward converters. The fly-forward converters with two inductors input and output, that output current is consistent but excessive switching losses [52]. The fly-forward converters with two inductor inputs and output with diode-capacitor boosters have continuity of the converter output current and high voltage gain, but reduce the converter efficiency through hard switching [53].

The fly-forward converters are divided into the output voltage. In these topologies there has been constant output current of the converter and low stress voltage on the main switch and other elements of the converter [54].

The converters with different topologies and soft switching methods have been used in various studies [55]. The loss energy of the converter switches off is stored in the capacitor of the snubber circuit. The energy stored in the capacitor of snubber circuits will be returned to the converter by an active circuit. In this topology, the energy recovered from the snubber capacitor is reused by the converter or is added at the input of the next layer [56]. The converters with a passive snubber circuit to reduce switching losses are used to recover the energy stored in the converter snubber capacitor [57]. The energy stored in the snubber capacitor is often lost or returned to the converter by techniques such as coupled inductors. This method has increased the volume, cost, number of elements and complexity of the converter.

The topology in [58] is used to improve efficiency and reduce switching losses. The auxiliary capacitor is used as a snubber by an active switch. The energy stored in the auxiliary capacitor is returned to the converter. In [59] active clamp snubber circuit is practical but has been used with a complex control circuit. This method has increased

the number of elements and the complexity of the circuit to improve the efficiency of the converter.

In this paper, a new boost converter has created a proposed topology. The proposed converter combines the topologies of a conventional boost converter and a boost fly-forward converter. This converter reduces switching losses with an active snubber circuit. The energy of the converter switching losses, stored in the active snubber capacitor, is returned to the converter. The converter had high voltage gain and low switching losses. The proposed converter had a high voltage gain by combining two boost topologies and a low loss power with an active snubber circuit. The proposed active snubber circuit was able to reduce switching losses and store this energy in the capacitor. The energy stored in the active snubber capacitor is returned to the converter in a simple way. The proposed boost converter will have a high output voltage and high efficiency with the technique of reducing the switching losses of the active snubber circuit. The PSPICE software was used to simulate the proposed converter because it is possible to model the elements with their real characteristics. In other words, it does not simulate the equipment ideally. Therefore, the construction time will be the least problem and the simulation and practical results will overlap to an acceptable extent.

The structure of the paper is as follows. After stating the problem in the previous section, the structure of the converter is described in section 2. Converter operation modes are presented in section 3. Operation states are evaluated in section 4. The simulation results are shown in section 5. Laboratory samples made are presented in section 6. Finally, the conclusion is stated in section 7.

2. Converter Structure

In this paper, a new structure of non-isolated boost converters is proposed. This topology combines the two structures of a conventional boost converter and a fly-forward boost converter. Such a step-up converter increases the output voltage with an acceptable voltage gain. In this topology, a new technique is used as an active snubber circuit with energy recovery capability to reduce switching losses. The most important task of the snubber circuit used in most boost converters is to reduce switching losses from the moment the shutdown command arrives at the main switch until the main switch is completely turned off.

The active snubber with the desired energy recovery capability has reduced the loss of turning

off the main switch, and on the other hand, the significant amount of power stored in the capacitor of the active snubber circuit, with a simple and practical technique, is delivered to the converter and finally converted into useful power to the output of the converter. This active snubber circuit as an auxiliary structure has increased the efficiency of the converter, because in most of the structures using the snubber circuit, the power stored in the snubber capacitor is wasted as losses on the switch. The snubber circuit reduces the pressure on the main switch by reducing the switching losses, while the active snubber topology with the ability to recover the energy stored in the snubber capacitor makes it possible to increase the transmission power of the converter without adding another power switch. In boost converters, checking the switching losses on the main switch is one of the basic and important parameters. A large part of switching losses in boost converters arise in a general mode. It also means that the drain-source voltage of the main switch of the converter is not zero and at the same time the current is flowing from the main switch of the converter.

One of the best techniques to reduce these losses is to reduce to zero or significantly reduce one of the loss factors, namely voltage or current or both. As mentioned so far, the switching loss is directly dependent on the time delay in turning on or off the main switch of the converter, which results in the non-zero parameters of the switching loss.

In the active snubber circuit with energy recovery capability, with accurate timing between turning off the main switch and turning on the snubber switch, the flow path through the snubber circuit is guaranteed until the main switch of the converter is completely turned off. This technique causes the main switch drain-source voltage to be minimized due to the snubber capacitor. This function is similar to conventional snubber circuits where the energy converted to losses when turned off on the main switch of converter is stored in the snubber capacitor. In the next step, when the snubber switch is turned off, the energy stored in the snubber capacitor, which in most of the normal snubber circuits is converted into losses in the next cycle on the main switch, is returned through the snubber diode to be restored to the converter inductor. In this structure, the voltage continuity of the capacitor minimizes the losses of the main switch of the converter at the time of shutdown. Also, keeping the current of converter inductors current through the snubber circuit has largely prevented voltage spikes and imposed voltage stress on the main switch of the converter.

The snubber circuit switch flows the current, until the current of the main switch of the converter is zero. It should be known that the snubber circuit is widely used in boost converters, but the new snubber circuits have been given a lot of attention, preventing the loss of energy stored in the capacitor of the snubber circuit. This demand has been well realized by using the active snubber circuit with the ability to recover the energy stored in the snubber capacitor. The fly-forward converter covers two modes of operation. In the first mode, the forward inductor feeds the output current until it directs the main switch of the converter. The second mode of self-fly-back supplies the load when the main switch of the converter is turned off.

This topology uses a non-isolated fly-forward converter paralleled with a conventional boost converter as shown in Fig. 1. High efficiency, low voltage stress on circuit elements and acceptable transmission power with only one powered switch are the strengths of the proposed topology. On the other hand, the fly-forward part guarantees the continuity of the current of the converter as well as the increase of the flexible voltage gain of the receiver by changing the conversion ratio of the fly-forward circuit according to the place of use of the converter and the desired output voltage.
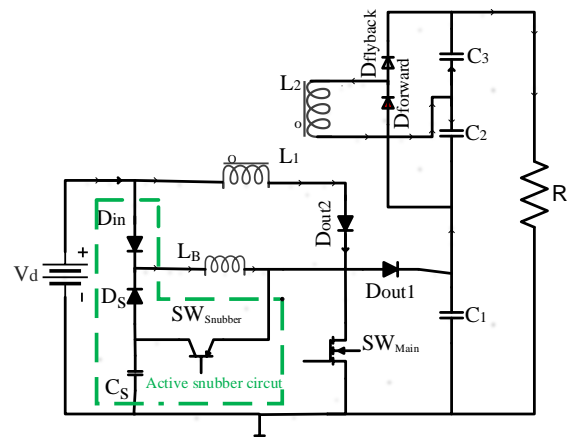

Figure 1. Proposed converter circuit

3. Operation Modes

The proposed converter includes four operating modes. D_1 is the main switch duty cycle, D_2 is the snubber switch duty cycle and n are the conversion ratio of the fly-forward converter [23].

$$\begin{cases} n = \dfrac{N_2}{N_1} \\[2mm] D_1 = \dfrac{t_{on}^{SWmain}}{T} \\[2mm] D_2 = \dfrac{t_{on}^{SWsnuber}}{T} \\[2mm] t_{discharge}^{Cs} = 4D_2 = t_{rV} \end{cases} \qquad (1)$$

3.1. Mode 1 [t₀, t₁]

As observed in Fig. (2-a), the period turned is within [t_0, t_1] the main switch, and D_{in}, D_{out2}, and $D_{Forward}$ diodes are guided and D_s, D_{out1} and $D_{flyback}$ diodes are turned off. The snubber switch, $SW_{snubber}$, is turned off. In this period, the L_1 and L_B inductors are charged. The C_2 capacitor is charged through $D_{Forward}$ that directly biased diode and the converter output voltage supplied by C_1 and C_3 capacitors.

The inductor L_B is related to the conventional boost converter, the inductor L_1 is the primary inductor of the coupling branch, the C_2 is the capacitor output part forward of the converter and L_2 is the secondary coupling of the converter. V_d is the input DC voltage of the converter. The conventional equation for calculating the range of inductance changes without saturation in converters is proportional to the duty cycle, input voltage and reverse inductance of the inductance. The following equations are given for this time period [31]:

$$(\Delta i_{L1})_{on}^{SWmain} = \frac{D_1 T V_d}{L_1} \qquad (2)$$

$$V_{C2} = nV_d \qquad (3)$$

$$v_{Cs}(t) = V_d \qquad 0 \le t < D_1 T \qquad (4)$$

$$i_{Cs}(t) = 0 \qquad 0 \le t < D_1 T \qquad (5)$$

3.2. Mode 2 [t₁, t₂]

At the beginning of this state, as soon as the main switch is turned off, the snubber switch is turned on. The diode situation is similar to that of state one. As observed in Fig. (2-b), the inductors L_1 and L_B are being charged, while inductors L_2 in this period is directly biased through $D_{forward}$, and in t_f, next to charging the C_2 capacitor through C_1 and C_3 capacitors, provides the regained energy load. The relationships of this time period are described in (6) and (7):

$$(\Delta i_{L1})_{on}^{SWsnubber} = \frac{D_2 T (V_d - V_{Cs})}{L_1} \qquad (6)$$

$$V_{C2} = nV_d \qquad (7)$$

For the snubber capacitor, there will be the following equations:

$$i_{SWmain}(t) = (I_{LB} + I_{L1})(1 - \frac{t}{t_f}) \quad for \ \ D_1 T \le t < t_f \qquad (8)$$

$$i_{Cs}(t) = (I_{LB} + I_{L1}) \qquad D_1 T \le t < t_f \qquad (9)$$

$$v_{Cs}(t) = \frac{1}{c} \int_0^t \frac{(I_{LB} + I_{L1})t}{t_f} = \frac{(I_{LB} + I_{L1})t^2}{2C \times t_f} \quad D_1 T \le t < t_f \qquad (10)$$

$$(\Delta i_{LB})_{off}^{SW(main,snubber)} = \frac{(V_{Cs} - V_{C1})(4D_2)T}{L_B} \qquad (11)$$

Equation (12) shows how the inductor charges the snubber capacitor according to the continuity of its current. This is confirmed by the increase in the voltage of the snubber capacitor, where the t_f is the time delay between turning off the main converter switch and zero current. The t_{rV} is a charging time snubber capacitor.

3.3. Mode 3 [t₂, t₃]

The snubber switch turns off the moment t_2, the $D_{forward}$ diode turns off, and the $D_{flyback}$, D_s, and D_{out1} diodes turn on. The flow path in this mode is shown in Fig. (2-c). In this mode, the time interval [t2, t3], the voltage and current relations of the inductors L_1, L_2 and L_B can be determined as follows [31]:

$$(\Delta i_{LB})_{off}^{SW(main,snubber)} = \frac{(V_{Cs} - V_{C1})D_{Cs}T}{L_B} \qquad (13)$$

$$V_{L1} = -\frac{N_1}{N_2} V_{C3} \qquad (14)$$

$$(\Delta i_{L1})_{off}^{SW(main.snubber)} = \frac{D_{Cs}T(-V_{C3}(\frac{N_1}{N_2}) - V_{Cs})}{L_1} \qquad (15)$$

$$v_{Cs}(t) = [\frac{1}{C_s} \int_{t_f}^t (I_{LB} + I_{L1})] + v_{Cs}(t_f)$$

$$\Rightarrow v_{Cs}(t) = \frac{(I_{LB} + I_{L1})}{C_s}(t - t_f) + \frac{(I_{LB} + I_{L1})t_f}{2C_s}(t_f \le t < t_{rV}) \qquad (16)$$

3.4. Mode 4 [t₃, t₄]

In this mode, both the active converter switches and the $D_{forward}$ turn off. The $D_{flyback}$, D_s and D_{out1} are turned on. The stored energy of the snubber capacitor is converted to the output, and the voltage of the snubber capacitor decreases, to the extent that it is less than the input voltage. When the snubber capacitor voltage drops below the converter input voltage, the D_{in} diode turns on and the D_s diode turns off. Converter current conduction is shown in Fig. (2-d). Based on the stated content and considering the formulas and analysis of Fig. (2-d), we will have [31]:

$$(\Delta i_{LB})_{off}^{SW (main ,snubber)}$$

$$= \frac{(V_d - V_{C1})(1 - (D_1 + D_2 + D_{Cs}))T}{L_B} \quad (17)$$

$$v_{Cs}(t) = V_d \qquad t_{rv} \leq t < T \quad (18)$$

$$i_{Cs}(t) = 0 \qquad t_{rv} \leq t < T \quad (19)$$

$$(\Delta i_{L1})_{off}^{SW (main.snubber)}$$

$$= \frac{(-V_{C3}(\frac{N_1}{N_2}) - V_{C1})(1 - (D_1 + D_2 + D_{Cs}))T}{L_1} \quad (20)$$
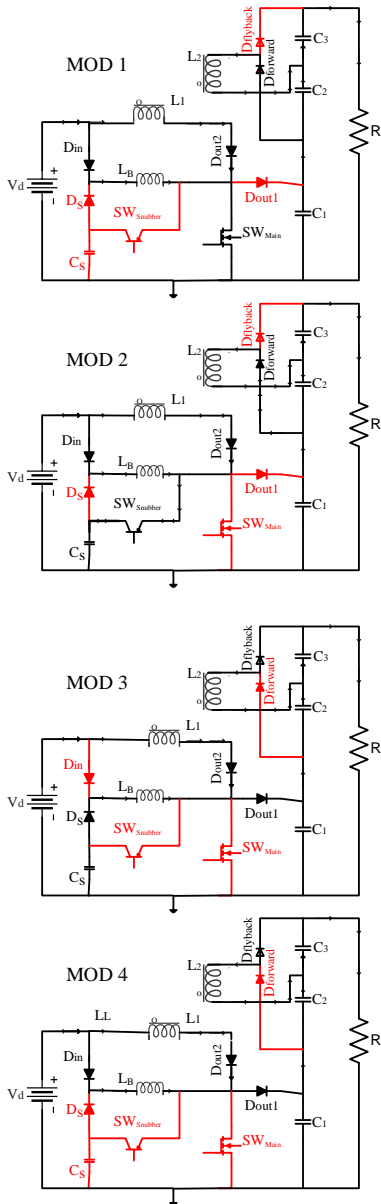

Figure 2. The modes of the proposed converter

4. Steady State Assessment

According to the operating modes of the proposed converter, in this section, the steady state of the converter is investigated. The voltage gain is calculated as one of the most important parameters of a boost converter.

In this section, all converter elements are considered ideal. It should be known that in order to prevent the inductor from breaking, the algebraic sum of the inductor's charging and discharging current must be zero. Based on this important principle, it is possible to consider the foundation of calculations of other parameters. The proposed circuit in steady state gives converter modes:

$$(\Delta i_{LB})_{on}^{SWmain} + (\Delta i_{LB})_{on}^{SWsnuber}$$
$$+ (\Delta i_{LB})_{off}^{SWmain} + (\Delta i_{LB})_{off}^{SWsnuber} = 0 \quad (21)$$

$$V_{Cs} = \frac{1}{(1 - D_2)} V_d \quad (22)$$

$$V_{C1} = \frac{1 - D_2(1 - 4D_2)}{1 - (D_1 - D_2)} V_d \quad (23)$$

$$V_{C2} = nV_d \quad (24)$$

$$V_{C3} = (\frac{D_1 - (5D_2)}{(1 - (D_1 + D_2))}) nV_d \quad (25)$$

$$V_{out} = V_{C1} + V_{C2} + V_{C3} \quad (26)$$

$$V_{out} = [\frac{1 - D_2(1 - 4D_2)}{1 - (D_1 - D_2)}$$
$$+ n + (\frac{D_1 - (5D_2)}{(1 - (D_1 + D_2))}) n] V_d \quad (27)$$

$$M_V = \frac{V_{out}}{V_d} \rightarrow M_V = \frac{1 - D_2(1 - 4D_2)}{1 - (D_1 - D_2)}$$
$$+ n + (\frac{D_1 - (5D_2)}{(1 - (D_1 + D_2))}) n \quad (28)$$

$$M_V = \frac{1 + n(1 - 6D_2) + D_2(4D_2 - 1)}{1 - (D_1 + D_2)} \quad (29)$$

where, as observed, this converter, though with a low conversion ratio and limited operation period, has a proper voltage gain coefficient. As to power and predicted features like the output capacitor voltage ripple and the converter inductor's current ripple at the system's loaded state, the converter inductors and capacitors are designed based on the design requirements. To design the L_B inductor as an equation related to a simple boost converter constant current state [33]:

$$L_B = \frac{D_1 V_d}{f_s \times \Delta I_{LB}} \quad (30)$$

Similarly, for a continuous current fly-back converter [33]:

$$L_1 = \frac{(D_1 + D_2)V_d}{f_s \times \Delta I_{L1}} \quad (31)$$

$$L_2 = n^2 \times L_1 \quad (32)$$

where n is the ratio, D_1 is the duty cycle of the main converter switch converter, D_2 is the duty cycle of the snubber switch, $I_{O,\,max}$ is the highest input current, V_d is the input switching voltage, f is the switching frequency and ΔI_{L1} is the primary coupled current ripple. The output capacitors of the converter. Their value is calculated in such a way where Δv_C is the output voltage ripple of the output capacitors converter [45]:

$$C_1 = \frac{(D_1 + 5D_2)I_{O,max}}{f_s \times \Delta v_{C1}} \quad (33)$$

$$C_2 = \frac{(1-(D_1 + 5D_2)\times I_{O,max}}{f_s \times \Delta v_{C2}} \quad (34)$$

$$C_3 = \frac{(D_1 + D_2)I_{O,max}}{f_s \times \Delta v_{C3}} \quad (35)$$

The snubber capacitor converter is calculated as follows [13]:

$$V_{Cs}(t) = \begin{cases} \dfrac{1}{C_S}\int_0^t \dfrac{(I_{LB}+I_{L1})}{t_f} = \dfrac{(I_{LB}+I_{Li})t^2}{2C_S\,t_f} \\ \qquad\qquad for\, D_1 T \le t < t_f \\[4pt] \dfrac{1}{C_S}\int_{t_f}^t (I_{LB}+I_{L1}) + v_{C_S}(t_f) \\ \qquad = \dfrac{(I_{LB}+I_{Li})}{C_S}(t-t_f) \\[4pt] \qquad + \dfrac{(I_{LB}+I_{Li})t_f}{2C_S}\, for\, t_f \le t < t_W \\[4pt] V_d\, for\, t_f \ge t_W \end{cases} \quad (36)$$

$$C_s = \frac{I_{max}^{SWmain} \times t_f}{2V_f} \quad (37)$$

$$P_{Cs}^{t_f} = \frac{1}{2}f_s C_s V_{Cs}^2$$
$$= \frac{1}{2}f_s C_s \left[\frac{(I_{LB}+I_{L1})t_f}{2C_s}\right]^2 \quad (38)$$
$$= \frac{[(I_{LB}+I_{L1})t_f]^2 f_s}{8C_s}$$

$$P_{Cs}^{t_{rV}} = \frac{1}{2}f_s C_s V_{Cs}^2$$
$$= \frac{1}{2}f_s C_s \left(\frac{I_{LB}t_f}{2C_s}\right)^2 = \frac{(I_{LB}\times t_f)^2 f_s}{8C_s} \quad (39)$$

$$P_{Cs}^{t_{rV}} = P_{Cs}^{t_f} \Rightarrow t_{rV} = \left(\frac{I_{LB}+I_{L1}}{I_{LB}}\right)t_f \quad (40)$$

where, t_f is the time it takes for the current to pass through the main converter switch to zero, t_{rV} is the charging or discharging time of the snubber capacitor.

Note, these two parameters are the intrinsic properties of each switch. The necessary factors influencing the switching losses and Pswmain indicate the energy losses of the main switch of the converter in the off state. The I_{max}^{SWmain} is the main switch, maximum converter current. The V_f is the maximum voltage snubber capacitor. In non-isolated converters, with increasing output voltage of the converter, the voltage stress on the components increases, especially on the main switch of the converter. Therefore, the boost converters, in addition to the voltage gain, the reduction of voltage stress is based on the converter components and especially the converter switches and the output diodes of the converter. High voltage stress on the converter components and high reverse break voltage components should be used. The use of devices with high reverse break voltage has a detrimental effect on the efficiency and productivity of the converter. The inverse voltage brake switch and the diodes are calculated and predicted as follows:

$$V_{off}^{SWmain} = V_{on}^{Dout1} + V_{C1}\, \square\, V_{C1}$$
$$\Rightarrow V_{off}^{SWmain} = \left(\frac{1-[D_2(1+D_2)-4D_2^2]}{1-(D_1+D_2)}\right)V_d \quad (41)$$

$$V_{off}^{SWsnubber} = V_{Cs} - V_d = \frac{(I_{LB}+I_{L1})t^2}{2C_s \times t_f} - V_d \quad (42)$$

$$V_{off}^{Dout1} = V_{C1}$$
$$\Rightarrow V_{off}^{SWmain} = \left(\frac{1-[D_2(1+D_2)-4D_2^2]}{1-(D_1+D_2)}\right)V_d \quad (43)$$

$$V_{off}^{D_{forward}} = V_{L2} + V_{C2}$$
$$\Rightarrow V_{off}^{D_{forward}} = \left[\left(\frac{D_1-5D_2^2}{(1-(D_1+D_2))}\right)+1\right]nV_d \quad (44)$$

$$V_{off}^{D_{flyback}} = V_{off}^{D_{forward}} \quad (45)$$

In the proposed converter, the voltage stress on the converter diodes and the converter switches is accepted. In this converter, the voltage across the

switch is less than half the output voltage of the converter, which is acceptable for a non-isolated boost converter. The contents of the proposed converter, it seems, compared to the converters presented based on non-isolated topologies, the converter is suitable in terms of voltage gain and voltage stress on the converter components accor-ding to the number of active converter switches.

The proposed converter features are compared to several non-isolated boost converters that are the basis of many boost converter designs. This comparison in terms of converter voltage gain factor, transducer power, voltage stress on the main switch of the converter, number of active converter switches and soft switching is shown in Table 1. Next, a 500-watt converter with a 48-volt input voltage is designed based on what has been described so far. For n=2, the voltage gain is:

Table 1. Main parameters of several converters with proposed topology

Structure \ Factor	Voltage gain	Voltage tension on the switch	Soft switching	Input/output voltage (v)	Switching frequency (Hz)/(w)	Maximum efficiency (%)
Converter consisting of two interleaved and intercooled boost converter cells [16]	$\dfrac{1}{1-(D_1+D_2)}$	V_o	--	30/67	50/100	87.5
Converter with coupled inductor suitable for renewable applications [17]	$\dfrac{n+1}{1-D}$	$\dfrac{V_o}{n+1}$	ZCS	20/200	25/200	95.8
interleaved high step-up converter [23]	$\dfrac{2(n+1)}{1-D}$	$\dfrac{V_o}{2(n+1)}$	ZCS-ZVS	48/480	50/580	94
Switched-Capacitor Based High Step-Up [28]	$\dfrac{2+nD+n}{1-D}$	$\dfrac{V_o}{2+nD+n}$	--	40/520	20/250	95.5
Converter with coupled output inductor with clamped circuit [60]	$\dfrac{1+nD}{1-D}$	$\dfrac{nV_o}{1+nD}$	--	75/400	100/1000	92.3
Converter with an output coupled inductor and active clamped circuit [61]	$\dfrac{1+nD}{1-D}$	$\dfrac{(1+n)V_o}{1+nD}$	At ON instance	25~40/400	66/200	92

Combined converters with fly-back structure [62]	$\dfrac{1+nD}{1-D}$	$\dfrac{nV_o}{1+nD}$	--	75/380	100/300	92.4
Proposed structure	$\dfrac{1-[D_2(1-2D_2)]}{M_V[1-(D_1+D_2)]}V_o$	$\dfrac{1-[D_2(1-2D_2)]}{M_V[1-(D_1+D_2)]}V_o$	At ON instance	48/380	100/500	95.45
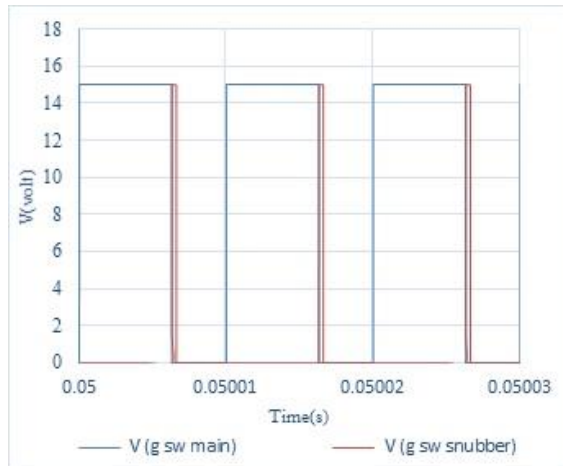
(a) The main switch control signals of the converter and the snubber circuit switch.
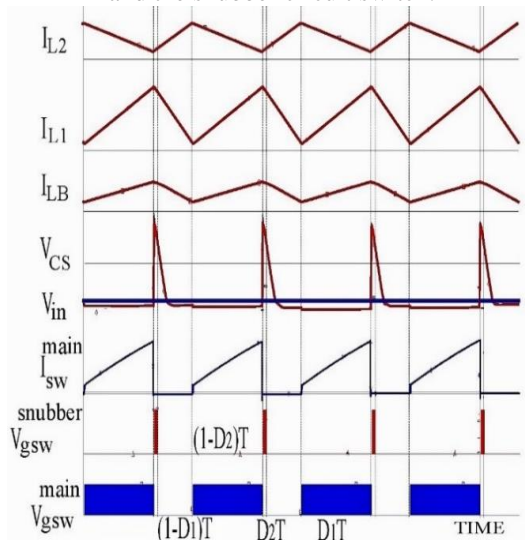

(b) The main waveform proposed converter

Figure 3. The waveform corresponds to the main converter drive switch and the snubber circuit switch

$$M_V = \frac{V_{out}}{V_d} = \frac{380}{48} = 7.92 \qquad (46)$$

$$\eta = \frac{[(V_{C1}+V_{C1}+V_{C1})\times I_R] + (\dfrac{[(I_{L1}+I_{LB})t_f]^2 \times f_S}{8C_S})}{[(I_{L1}+I_{LB})\times V_d]} \qquad (47)$$

1425

Showing the converter efficiency in (46). This equation clearly shows the effect of increasing efficiency on energy recovery through the active snubber circuit. The recovered energy of the snubber circuit capacitor and its conversion to useful power has confirmed the capability of the proposed topology in improving the efficiency of the converter. The converter switches are managed by a precise and reliable control circuit. The control structure of the proposed converter is designed as a laboratory sample in an open loop structure and the load is considered constant. This control circuit consists of a programmable part in order to make two separate control commands, one of which controls the main switch of the converter and the other one controls the switch of the snubber circuit. To ensure the correct and error-free operation of the control structure, the built-in timers of the microcontroller are used. The control signal made by the microcontroller from the optical isolation power section is amplified and de-noised with conventional techniques as well as protected against possible environmental and magnetic noises. Finally, a control signal is applied to each of the switches with the appropriate voltage and current and precise timing.

The discussed control circuit provides a control signal for the master switch drive. The width of the signal sent to keep the main switch on is determined by each consumer and the duty cycle desired by the user according to the output voltage and output power. Next, at exactly the same time as the main switch is turned off, the converter sends the turn-on signal to the snubber switch. The snubber switch current flow time is considered equal to the switch off time delay of the main converter switch. The control section of the proposed converter, including the oscillator section and the diversion gate section. Of course, it should be noted that this structure has been analysed and opened as an open circuit. The basis of the control section is that a signal with a changeable duty cycle is made and, with the help of an isolated power supply and a gate driver class, the main switch for the converter is made. Now, with the help of one of the internal timers of the microcontroller, which produces the main signal, a fixed width signal is created, the time of which is considered as long as the main switch of the converter is turned off. Another microcontroller pin transmits the signal generated by the snubber circuit to a power supply and a separate data gate to drive the active snubber circuit switch

The schematic and sample waveform as a control signal is shown in Fig. (3-a). The main waveform for this topology includes the inductor current, and snubber capacitor voltage is diagrammed Fig. (3-b).

5. Simulation Results and Discussion

The proposed converter is simulated by P-Spice software to ensure the correct performance in a steady state. In this section, for the purpose of simpler analysis, the converter inductors are considered ideal. To model the magnetic coupling of fly-forward topology, we used a magnetic coupler considering leakage flux. The simulation results of the proposed converter in PSPICE software are shown in Fig. 4.
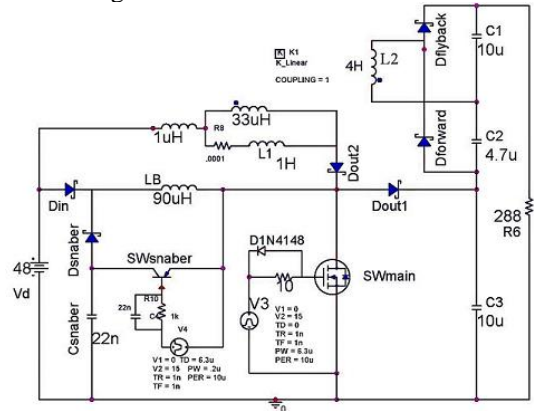

Figure 4. The proposed converter in PISPIS s/w environment

In the presented topology, two widely used structures of boost converters are combined: the branch without magnetic coupling of a conventional boost converter and the branch with magnetic coupling of a fly-forward converter. The conventional boost converter helps in increasing the voltage and feeding the load and is effective in recovering the energy stored in the snubber capacitor of the active snubber circuit. In addition to providing the output load and improving the voltage gain of the converter, the fly-forward converter has helped the continuity of the converter current.

The PSPICE software was used to simulate the proposed converter because it is possible to model the elements with their real characteristics. In other words, it does not simulate the equipment ideally. Therefore, the construction time will be the least problem and the simulation and practical results will overlap to an acceptable extent. The desired structure with this arrangement has caused the converter to be within the acceptable range in terms of basic parameters such as voltage gain, efficiency, transmission power, controllability, voltage stresses on the converter elements, especially switches and

diodes, and not adding the number of power switches. The proposed converter can be used in most local power plants with different characteristics, including solar power plants, combined fuel cell/battery power plants.

Another advantage of the proposed structure is the output voltage obtained from the summation of the voltage of the three capacitors that are connected in series at the output. The technique of putting several capacitors in series at the output, the maximum reverse voltage applied to the power switch is limited to the voltage of the output capacitor corresponding to the normal boost converter (C3) and makes it possible to use power switches with lower reverse breakdown voltage and lower conduction resistance. On the other hand, connecting several capacitors in series at the output will reduce the current stress of the output capacitors of the converter. When the main switch is turned on, the transformer inductor starts charging and when the switch is turned off, this energy will be delivered to the output. This charge and discharge will be completely continuous and will not have any jumps. The current waveform of the fly-forward converter branch, is shown in Fig. 5 and the typical boost branch inductor current waveform is in Fig. 6.

Fig. 7 shows the gate control signal of the main switch of the converter and the voltage of the snubber capacitor to prove the correct operation of the active snubber circuit and the charging of the snubber capacitor exactly at the same time as the main switch of the converter is turned off. The drain-source voltage of the main switch is shown in Fig. 8. At the same time as the main switch is turned off and the switch to the active snubber circuit is turned on, the voltage of the snubber capacitor increases, which can confirm the correct operation of the active snubber circuit.

The results of the calculations and simulations are a conversion ratio of n=2. The dependence of voltage gain on duty cycle in several conversion ratios is shown in Fig. 9.

6. Experimental Results

In this section, a laboratory sample is made from the proposed converter. A detailed design is performed for the laboratory sample, according to the simulation results and the expressed formulas.
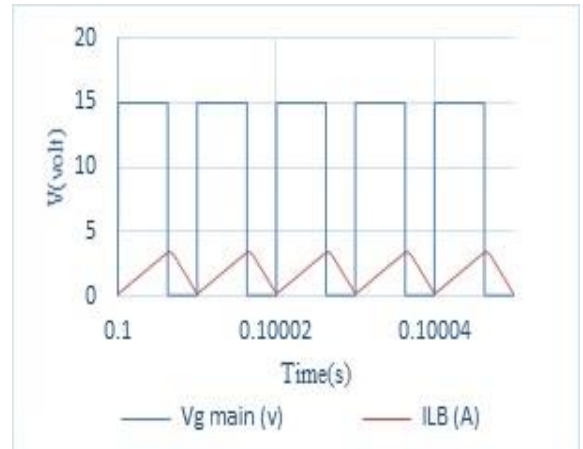
Figure 5. Initially coupled inductor-current (L_2)
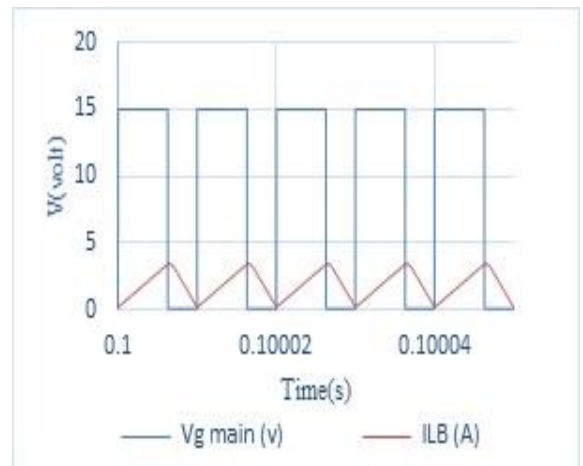
Figure 6. Non coupled inductor-branch current (L_B)
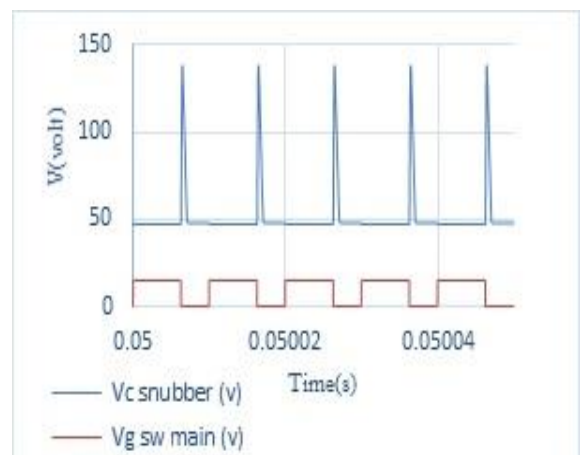
Figure 7. The main gate switch voltage and the capacitor SNUBBER voltage
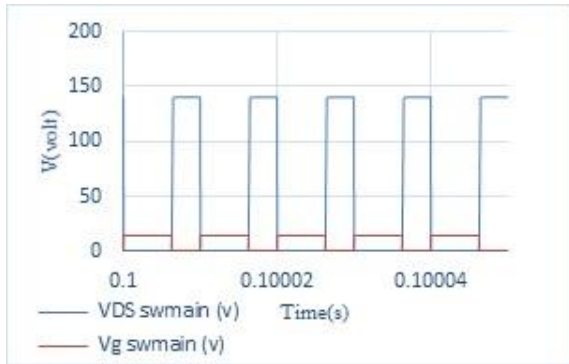
Figure 8. The D-S of main switch voltage
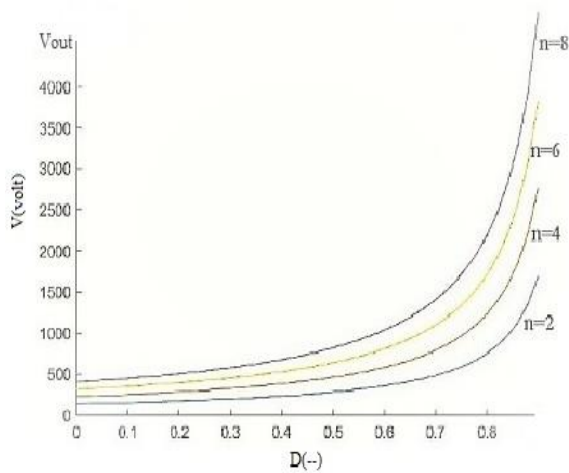
Figure 9. Output voltage based on performance duration for different coupled ratios

In the proposed converter, using a magnetic coupling between a 33 (mH) inductor with a conversion ratio n=2 and a secondary inductor of 130 µH and the presence of a conventional boost converter with a 90 µH inductor (LB). In the construction of the converter, the MBR40250 diode is used, which is a fast diode with a reverse break voltage of 250 (v) and a maximum current of 40 (A). This diode is acceptable in terms of input bias voltage, which has caused the maximum power loss of the diode (Von is approximately 0.7). The SUM85N15-19 switch, the MOSFET power with a reverse break voltage of 150 (V), is used as the main switch and the 2SA1943 switch is used as the snubber switch. The operating frequency of this converter is 100 (kHz) and it is made at the power of 500 watts. For the converter input voltage, a direct current source of 50 (A) is used. The output voltage of the converter is set to 380 (v), the voltage gain is about 8. The specifications of the converter are given in Table 2. Laboratory sample of the proposed

converter, made in the Smart Microgrid Research Center, Najafabad Branch, Islamic Azad University, Iran. This converter example is shown in Fig. 10.
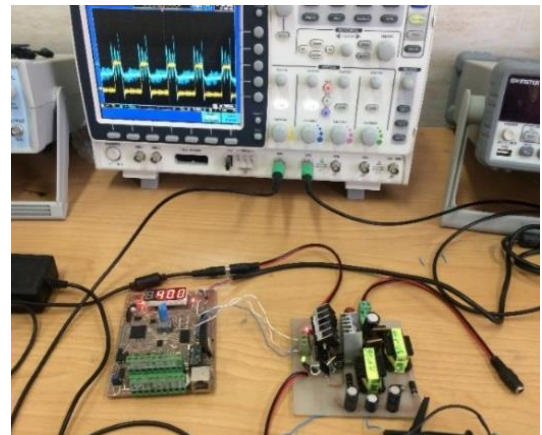

Figure 10. The constructed converter

Table 2. Features of converter tabulated

Quantity	Amount	Unit
V_{in}	48	V
V_{out}	385	V
P_{out}	500	W
M_V	8	-
R_{Load}	300	Ω
N	2	-
D_1	0.63	-
D_2	0.02	-

The elements used in the sample are given in Table 3. The diagrams of the diodes' voltage Dforward, Dflyback, Dout2 and Dout1 are drawn in Figs. 11. The voltage waveforms of inductors LB, L1, and L2 are shown in Figs. 12, 13, and 14. The snubber capacitor voltage is increased and the main converter switch is turned off. The snubber capacitor voltage wave VCs is shown in Fig. 15.

The snubber capacitor is charged when the main switch is turned off. The results of design, simulation and construction were compared in Table 4. Obviously, the important parameters of a boost converter were categorized for the proposed converter in this table. In this table, all design, simulation and practical results were confirmed. The parameters were compared for the proposed structure. This converter was identified in terms of transmission power and voltage gain.
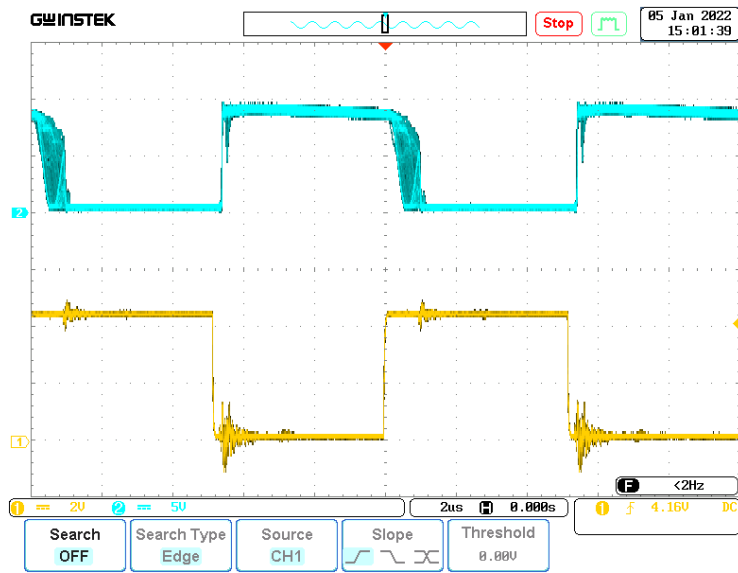
(a) The diode' voltage $D_{forward}$
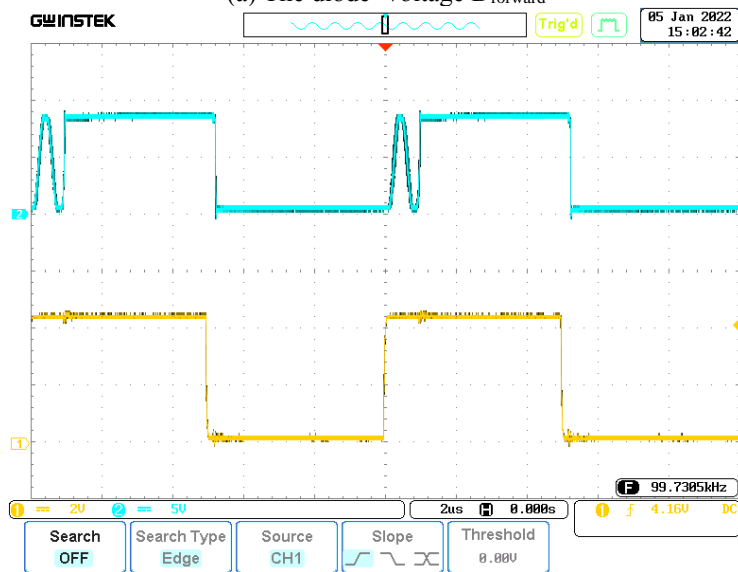
(b) The diode' voltage $D_{flyback}$
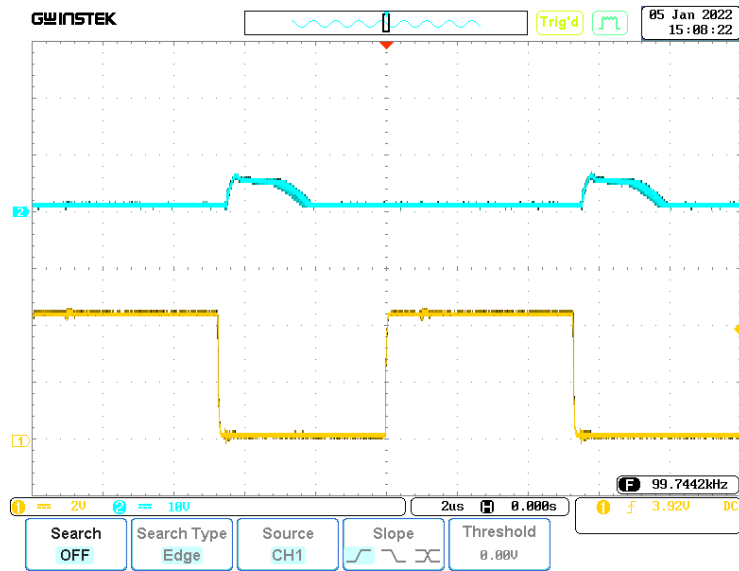
(c) The diode' voltage D_{out2}
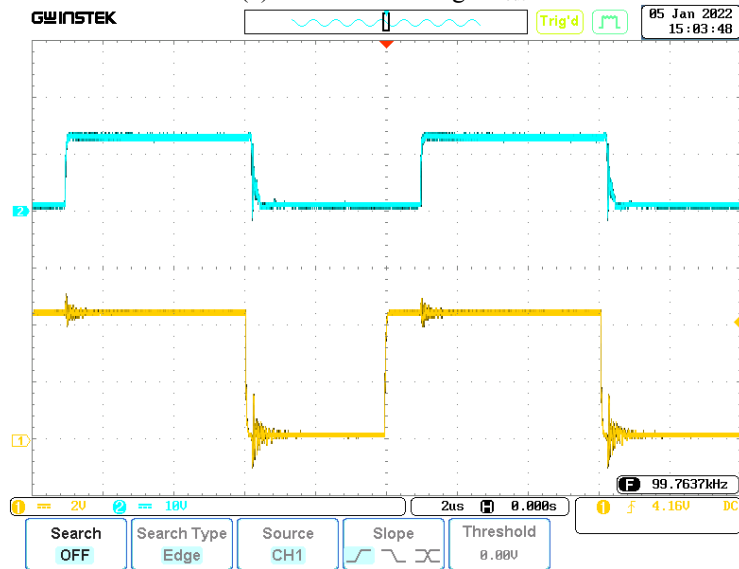
(d) The diode' voltage D_{out1}

Figure 11. The diodes' voltage $D_{forward}$, $D_{flyback}$, D_{out2} and D_{out1}

Table 3. Applied elements tabulated

Element type	Element number	The location used in the converter
C	10 uF (250v)	C_1, C_3
C	4.7 uF (250v)	C_2
Power switch	IRFP 260	Main switch
PNP BJT	SUM85N15-19	Snubber switch
C	22 nF	C_S
L	90 uH	L_B
L	33/130 uH	$L_{1/}$ L_2
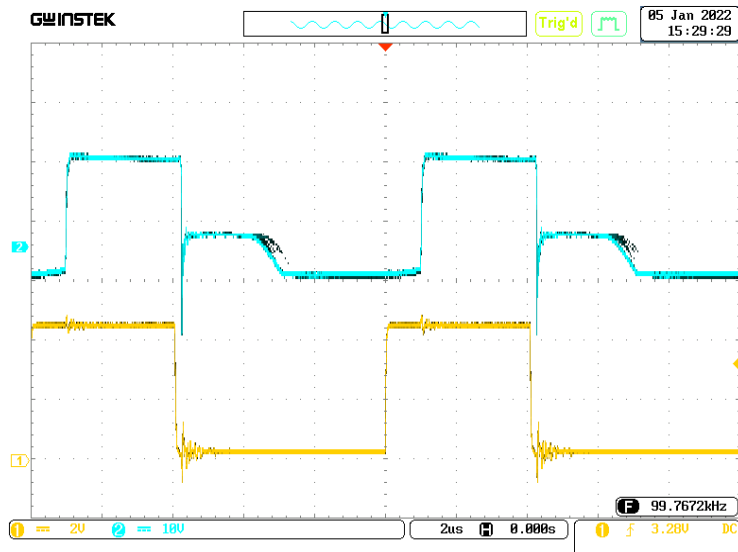
Figure 12. The voltage waveforms of inductors L_B
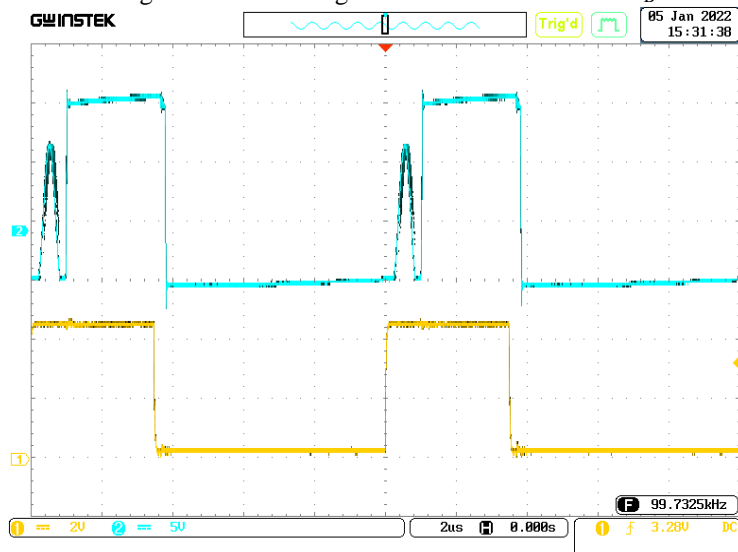
Figure 13. The voltage waveforms of inductors L_1

Table 4. Comparison of the results of design, simulation and implementation of the proposed converter

Proposed converter results	V_{C1} (v)	V_{C2} (v)	V_{C3} (v)	V_{out} (v)	M_V
Designed	167	85	142	394	8.2
simulation	157	88	140	385	8
Practical results	155	85	150	395	8.125
Error(S-P)%	1.3	3.4	6.7	2.5	1.5
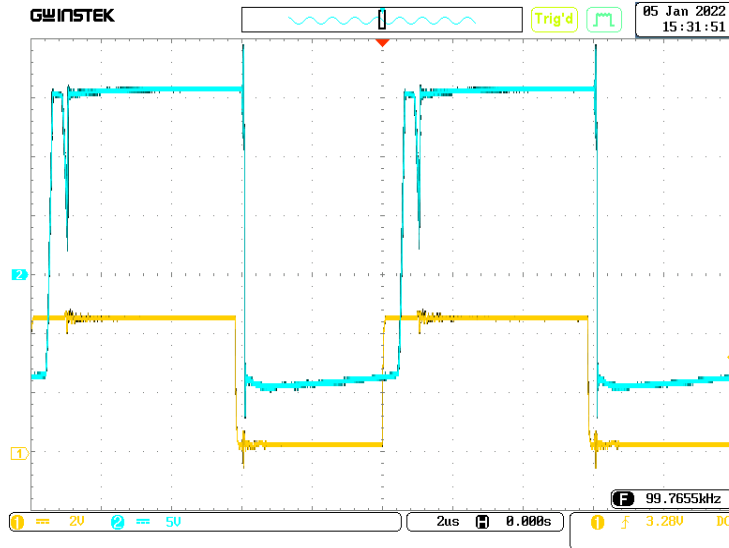
Figure 14. The voltage waveforms of inductors L_2
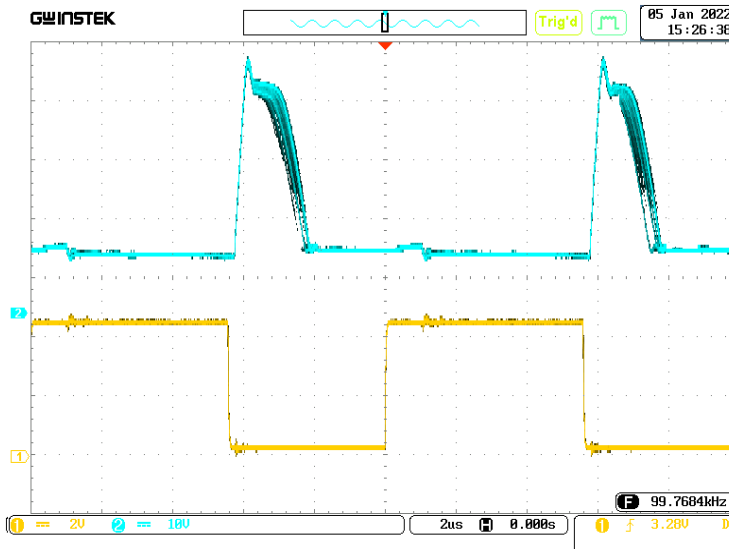
Figure 15. The Snubber capacitor voltage and the gate voltage of main switch

7. Conclusions

In this paper, the boost converter is proposed as the basic topology. The proposed basic topology is a combination of two boost converters: a conventional boost converter and a fly-forward converter. This purposeful combination has resulted in a boost converter with a suitable voltage gain and transmission power.

In addition, dividing the output voltage between the series capacitors has significantly reduced the voltage stress on the main switch and other converter elements. The fly-forward converter, in addition to being effective in voltage gain, has also helped the continuity of the converter current. These two parallel converters make it possible to transmit more power. The active snubber circuit with energy recovery capability reduces converter losses. In boost converters, most of the losses are caused when the main switch of the converter is turned off. Also, suddenly cutting the inductor current causes the inductor to react and create voltage spikes that may damage the circuit elements. The proposed snubber circuit has solved most of these problems.

The snubber capacitor will not allow a sudden increase in voltage at both ends of the main switch

of the converter due to the continuity of the capacitor voltage. In this way, the energy that was wasted on the main switch in normal structures is now stored in the snubber capacitor using this circuit. Then this energy is delivered to the converter as usable power. Such switching losses of the converter are reduced with the snubber circuit and the lost energy removed from the main switch of the converter is returned to the converter with the help of an active snubber circuit with the ability to recover energy. All these steps resulted in increasing the efficiency of the converter and reducing the switching losses. The important parameters of the proposed converter were compared with several well-known boost converters in Table 1.

The proposed structure is proposed for a specific converter. It is possible to check the performance of such a technique on other boost converters. Also, the performance of this structure should be discussed for converters with more than one active switch and multilayer converters. The timing and synchronization of the snubber circuit switch with the main switch of the converter is the most important part of the proposed topology and must be carefully analyzed and evaluated for other converters.

Nomenclature

N_1:	Number of primary fly-back wires.
N_2:	Number of secondary fly-back wires.
D_{out1}:	Conventional boost converter output diode.
D_{out2}	Fly-back boost converter output diode.
D_s	Active snubber circuit diode.
D_{in}	Converter input diode.
L_2	Secondary inductance of fly-back converter.
L_1	Primary inductance of fly-back converter.
M_V	Voltage gain of the converter.
D_1	The duty cycle of the main switch.
D_2	The duty cycle of the snubber circuit switch.
$D_{Forward}$	The output diode of the forward converter.
C_3	The output capacitor of the forward converter.
C_S	Active snubber circuit capacitor.
L_B	Conventional boost converter inductor.
$D_{flyback}$	The output diode of the fly-back converter

C_1	The output capacitor of the Conventional converter.
C_2	The output capacitor of the fly-back converter
$t_{disch\,arg\,e}^{Cs}$	Snubber capacitor charging time.
t_{rV}	The Snubber capacitor charging time.
I_{OMAX}	The main switch converter maximum current
V_f	The maximum voltage snubber capacitor
$P_{CS}^{t_{fv}}$	The power stored in the snubber capacitor during charging
V_d	The input switching voltage
$I_{O,\,max}$	The highest input current
f_S	The switching frequency
ΔV_C	The output voltage ripple of output capacitors converter
ΔI_{L1}	The primary inductor coupled current ripple
ΔI_{L2}	The secondary inductor coupled current ripple
ΔI_{LB}	The primary inductor Conventional boost current ripple

References

[1] Aryan Nezhad, M. (2022). Frequency control and power balancing in a hybrid renewable energy system (HRES): Effective tuning of PI controllers in the secondary control level. Journal of Solar Energy Research, 7(1), 963-970.

[2] Sharifiyana, O., Dehghani, M., Shahgholian, G., Mirtalaei, S.M.M., Jabbari, M. (2022). Overview of dc-dc non-insulated boost converters (Structure and improvement of main parameters). Journal of Intelligent Procedures in Electrical Technology, 12(48), 1-29.

[3] Haghshenas, G., Mirtalaei, S.M.M., Mordmand, H., Shahgholian, G. (2019). High step-up boost-fly back converter with soft switching for photovoltaic applications. Journal of Circuits, Systems, and Computers, 28(1), 1-16.

[4] Taghizadeh, S., Hossain, M.J., Lu, J., Water, W. (2018). A unified multi-functional on-board EV charger for power-quality control in household networks, Applied Energy, 215, 186-201.

[5] Bi, K., Liu, Y., Zhu, Y., Fan, Q. (2021). An impedance source modular DC/DC converter for energy storage system: analysis and design. International Journal of Electrical Power and Energy Systems, 133, 107261.

[6] Ceballos, J.P.V., Montoya, D.G., Ramos-Paja, C.A., Bastidas-Rodríguez, J.D. (2020).

Charger/discharger dc/dc converter with interleaved configuration for DC-bus regulation and battery protection", Energy Science and Engineering, 8(2), 530-543.

[7] Karimi, H., Jadid, S., Hasanzadeh, S. (2022). A stochastic tri-stage energy management for multi-energy systems considering electrical, thermal, and ice energy storage systems. Journal of Energy Storage, 55, 105393,

[8] Mallik, A., Al Nahian, S., Rashid, F. (2018). PV/T systems for renewable energy storage: A review. Journal of Solar Energy Research, 3(1), 35-42.

[9] Dhimish, M., Schofield, N. (2022). Single-switch boost-buck DC-DC converter for industrial fuel cell and photovoltaics applications. International Journal of Hydrogen Energy, 47(2), 1241-1255.

[10] Amir, A., Amir, A., Che, H.S., Elkhateb, A., Rahim, N.A. (2019). Comparative analysis of high voltage gain dc-dc converter topologies for photovoltaic systems. Renewable Energy, 136, 1147-1163.

[11] Wang, H., Gaillard, A., Hissel, D. (2019). A review of dc/dc converter-based electrochemical impedance spectroscopy for fuel cell electric vehicles. Renewable Energy, 141, 124-138.

[12] Rosas-Caro, J.C., Valdez-Resendiz, J.E., Mayo-Maldonado, J.C., Sanchez, V.M., Lopez-Nuñez, A.R., Barbosa, R., Valdivia, L.J., Fuel-cell energy generation system based on the series-capacitor boost converter. International Journal of Hydrogen Energy, 46(51), 26126-26137.

[13] Guilbert, A., Gaillard, A., N'Diaye, A., Djerdir, A. (2016). Power switch failures tolerance and remedial strategies of a 4-leg floating interleaved dc/dc boost converter for photovoltaic/fuel cell applications. Renewable Energy, 90, 14-27.

[14] Mirtalaei, M., Amani Nafchi, R. (2019). Boost high step-Up DC/DC converter with coupled inductors and diode-capacitor technique, Journal of Intelligent Procedures in Electrical Technology, 10(39), 3-12, 2019.

[15] Baddipadiga, B.P.R., Prabhala, V.A.K., Ferdowsi, M. (2018). A family of high-voltage-gain DC-DC converters based on a generalized structure. IEEE Trans. on Power Electronics, 33(10), 8399-8411.

[16] Spiliotis, K., Gonçalves, J.E., Sande, W.V.D., Ravyts, S., Daenen, M., Saelens, D., Baert, K., Driesen, J. (2019). Modeling and validation of a DC/DC power converter for building energy simulations: Application to BIPV systems. Applied Energy, 240, 646-665.

[17] Shojaeian, H., Hasanzadeh, S., Heydari, M. (2018). High efficient and high step-up dual switches converter based on three coupled inductors. International Journal of Industrial Electronics Control and Optimization, 1(2), 143-152.

[18] Sharifiyana, O., Dehghani, M., Shahgholian, G., Mirtalaei, S.M.M., Jabbari, M. (2023). Non-isolated boost converter with new active snubber structure and energy recovery capability. Journal of Circuits, Systems and Computers, 32(5), 2350084.

[19] Liu, H., Hu, H., Wu, H., Xing, Y., Batarseh, I., (2016). Overview of high-step-up coupled-inductor boost converters. IEEE Journal of Emerging and Selected Topics in Power Electronics, 4(2), 689-704.

[20] Samadi, M., Rakhtala, S.M., Ahmadian Alashti, M. (2019). Boost converter topologies, hybrid boost and new topologies of voltage multiplier in photovoltaic systems. Journal of Solar Energy Research, 4(4), 287-299.

[21] Gu, B., Dominic, J., Lai, J.S., Zhao, Z., Liu, C. (2012). High boost ratio hybrid transformer DC-DC converter for photovoltaic module applications. Proceeding of the IEEE/APEC, 598-606.

[22] Faiz, J., Shahgholian, G., Ehsan, M. (2008). Stability analysis and simulation of a single-phase voltage source UPS inverter with two-stage cascade output filter. European Transactions on Electrical Power, 18(1), 29-49.

[23] Lee, P.W., Lee, Y.S., Cheng, D.K., Liu, X.C. (2000). Steady-state analysis of an interleaved boost converter with coupled inductors. IEEE Trans. on Industrial Electronics, 47(4), 787–795.

[24] Pourjafar, S., Sedaghati, F., Shayeghi, H., Maalandish, M. (2019). High step-up dc–dc converter with coupled inductor suitable for renewable applications. IET Power Electronics, 12(1), 92-101.

[25] Lin, B.R., Chen, J.J. (2008). Analysis and impl-ementation of a soft-switching converter with high-voltage conversion ratio. IET Power Electronics, 1(3), 386–394.

[26] Taheri, D., Shahgholian, G., Mirtalaei, M.M. (2022). Analysis, design and implementation of a high step-up multi-port non-isolated converter with coupled inductor and soft switching for photovoltaic applications. IET Generation,

Transmission and Distribution, 16(17), 3473-3497.

[27] Huber, L., Jovanovic, M.M. (2000). A design approach for server power supplies for networking applications. Proceeding of the IEEE/APEC, 1163–1169.

[28] Tohidi, B., Delshad, M., Saghafi, H. (2022). A new interleaved zvt high step-up converter with low count elements for photovoltaic applications. Journal of Renewable Energy and Environment, 9(1), 70-77.

[29] M. Emamdad, Akbari, E., Karbasi, S., Zare Ghaleh Seyyedi, A. (2024). Design and analysis of a new structure for non-isolated dc-dc boost converters. Journal of Intelligent Procedures in Electrical Technology, 15(58), 109-120.

[30] Semeskandeh, S., Hojjat, M., Hosseini-Abardeh, M. (2024), Improving the efficiency of floating photovoltaic system in the northern part of Iran using a two-stage multi-string inverter, Journal of Intelligent Procedures in Electrical Technology, 15(57), 85-98.

[31] Law, K.K., Cheng, K.W., Yeung, Y.P. (2005). Design and analysis of switched-capacitor-based step-up resonant converters. IEEE Trans. Circuits Systems, 52(5), 1998–2016.

[32] Kianpour, A., Shahgholian, G. (2017). A floating-output interleaved boost DC–DC converter with high step-up gain. Automatika, 58(1), 18-26.

[33] Ismail, E.H., Al-Saffar, M.A., Sabzali, A.J., Fardoun, A.A. (2008). A family of single-switch PWM converters with high step-up conversion ratio. IEEE Trans. Circuits Systems, 55(4), 1159–1171.

[34] Heidari Beni, S., Mirtalaei, S.M.M., Kianpour, A., Aghababaei Beni, S. (2017). Design and improvement of a soft switching high step-up boost converter with voltage multiplier. IET Power Electronics, 10(15), 2163-2169.

[35] Wu, T.F., Tseng, S.Y., Hu, J.S., Chen, Y.M. (2006). Buck and boost derived converter for livestock/poultry stunning applications. Proceeding of the IEEE/APEC, 1530–1536.

[36] Wong, Y.S., Chen, J.F., Liu, K.B., Hsieh, Y.P. (2017). A novel high step-up dc-dc converter with coupled inductor and switched clamp capacitor techniques for photovoltaic systems. Energies, 10, 378.

[37] Wei, J., Xu, P., Wu, H., Lee, F.C., Yaa, K., Yee, M. (2001), Comparison of three topology candidates for 12V VRM. Proceeding of the IEEE/APEC, 245- 251.

[38] Wu, T., Lai, Y., Hung, J., Chen, Y. (2008). Boost converter with coupled inductors and buck-boost type of active clamp. IEEE Trans. on Industrial Electronics, 55(1), 154-162.

[39] Suriyakulnaayudhya, R. (2015). A high gain step-up fly boost converter for high voltage high power applications. Proceeding of the IEEE/EEEIC, 1268-1272.

[40] Chang, T., Wu, Y., Chang, C., Yang, J. (2012). Soft-switching boost converter with a flyback snubber for high power applications. IEEE Trans. on Power Electronics, 27(3), 1108-1119.

[41] Wu, B, Smedley, K. (2015). A new Isolated Hybrid Boosting Converter. Proceeding of the IEEE/APEC, 28-34.

[42] Zelnik, R., Prazenica, M. (2021). Snubber Design for Fly-back Converter. Proceeding of the ICE, 1-6, Palanga, Lithuania.

[43] Bohra, S., Sarkar, A., Anand, S. (2020). Low side switch based regenerative snubber circuit for fly-back converter. Proceeding of the IEEE/ECCE, 4802-4807.

[44] Chen, F., Amirahmadi, A., Batarseh, I. (2014). Zero voltage switching forward-flyback converter with efficient active LC snubber circuit. Proceeding of the IEEE/APEC, 2041-2047.

[45] Gaurav, N., Ray, S. (2017). Design of snubber circuit to minimize switching and conduction losses in boost converter. Proceeding IEEE/ICSTM, 470-476, Chennai, India.

[46] Lee, H., Yun, J. (2019). Quasi-resonant voltage doubler with snubber capacitor for boost half-bridge DC-DC converter in photovoltaic micro-inverter. IEEE Trans. on Power Electronics, 34(9), 8377-8388.

[47] Liang, T.J., Chen, S.M., Yang, L.S., Chen, J.F., Ioinovici, A. (2012). Ultra-large gain step-up switched-capacitor DC-DC converter with a coupled inductor for alternative sources of energy. IEEE Trans. on Circuit and System, 59(4), 864-874.

[48] Martiš, J., Vorel, P., Procházka, P. (2019). 12 kW Flyback Converter with a Passive Quasi-resonant Snubber. Proceeding of the IEEE/EDPE, 106-111.

[49] Lagap, T., Dimopoulos, E., Munk-Nielsen, S. (2015). An RCDD snubber for a bidirectional flyback converter. Proceeding of the IEEE/EPE, 1-10.

[50] Halder, T. (2012). An improved hybrid energy recovery soft switching snubber for the Flyback converter. Proceeding of the IEEE/PEDES, 1-6,.

[51] S. M. Tadvin, S. R. B. Shah, M. R. T. Hossain, "A Brief Review of Snubber Circuits for Flyback Converter", Proceeding of the IEEE/I2CT, pp. 1-5, June 2018.

[52] Liu, V.T., Zhang, L.J. (2014). Design of high-efficiency boost-forward-fly back converters with high voltage gain. Proceeding of the IEEE/ICCA, Taichung, 1061-1066.

[53] Toffoli, F.L., Pereira, D.C., Paula, W.J., Júnior, D.S.O. (2015). Survey on non-isolated high-voltage step-up dc–dc topologies based on the boost converter. IET Power Electronics, 8(10), 2044-2057.

[54] W. Yu, C. Hutchens, J.S. Lai, J. Zhang, G. Lisi, A. Djabbari, G. Smith, T. Hegarty. (2009). High-efficiency converter with charge pump and coupled inductor for wide input photovoltaic AC module applications. Proceeding of the IEEE/ECCE, 3895-3900, San Jose, CA, USA.

[55] Gopi, A., Saravanakumar, R. (2014). High step-up isolated efficient single switch dc-dc converter for renewable energy source. Ain Shams Engineering Journal, 5(4), 1115-1127.

[56] Benedetto, M., Bigarelli, L., Lidozzi, A., Solero, L. (2021). Efficiency comparison of 2-level sic inverter and soft switching-snubber SiC inverter for electric motor drives. Energies, 14, 1690.

[57] Zhang, F., Yang, X., Chen. W., Wang, L. (2020). Voltage balancing control of series-connected SiC MOSFETs by using energy recovery snubber circuits. IEEE Trans on Power Electronics, 35(10), 10200-10212.

[58] Babu, K.R., Ramteke, M.R., Suryawanshi, H.M., Kothapalli, K.R. (2020). High gain soft switched DC-DC converter for renewable applications. Proceeding of the IEEE/TPEC, 1-6, College Station, TX, USA.

[59] Ferencz, I., Petreus, D., Pătărău, T. (2020). Comparative study of three snubber circuits for a phase-shift converter. Proceeding of the IEEE/SPEEDAM, 763-768, Sorrento, Italy.

[60] Premkumar, M., Kumar, C., Anbarasan, A., Sowmya, R. (2020). A novel non-isolated high step-up DC-DC boost converter using single switch for renewable energy systems. Electrical Engineering, 102, 811–829.

[61] Zhang, L., Yang, X., Zheng, T.Q., Zhang, J. (2020). A Passive soft-switching snubber with energy active recovery circuit for PWM inverters. IEEE Access, 8, 100031-100043.

[62] Esfahani, S.N., Delshad, M., Mohammad, B.T. (2020). A new family of soft single switched dc-dc converters with lossless passive snubber. Majlesi Journal of Electrical Engineering, 14, 51- 59.